

# Numerical modelling for optimizing flow distribution inside an electrostatic precipitator

Shah M. E. Haque, M. G. Rasul, M. M. K. Khan, A. V. Deev, and N. Subaschandar

**Abstract**— The performance of Electrostatic precipitator (ESP) is significantly affected by its complex flow distribution arising as a result of its complex inside geometry. In the present study the gas flow through a lab-scale ESP is modelled numerically using computational fluid dynamics (CFD) technique to optimize the flow distribution inside the ESP. CFD code FLUENT is used to carry out the computations. Numerical calculations for the gas flow are carried out by solving the Reynolds-averaged Navier-Stokes equations coupled with the realizable K- $\epsilon$  turbulence model equations. In the simulation the perforated plates, used inside the ESP, are modelled as thin porous media of finite thickness with directional permeability. The results of the simulation are discussed and compared with laboratory measured data. The model was used to simulate an optimized flow inside the ESP. The model developed could be used as a novel tool to predict the effect of possible modifications made to the ESP design on the flow pattern.

**Keywords**— CFD, Electrostatic precipitator, Flow distribution, Fluent, Perforated plate, Turbulent flow.

## I. INTRODUCTION

Over recent years the particle emissions from process industries have been attracting more attention due to an anticipation of upcoming strict environmental protection agency (EPA) regulations. Industrial pollution can be controlled by energy recovery and conservation [1], replacing conventional industrial processes with continuous and energy

efficient systems [2], or performance optimization of the emission control devices [3]. Electrostatic precipitators (ESP) are the most widely used devices which are capable of reducing particle emission effectively from power plants and other process industries. The flow distribution within the ESP has been reported to have varying effects on its dust collection performance depending on the arrangements of major geometrical features inside an ESP. It is difficult to carry out detailed and reliable measurements of fluid flow inside an ESP as the geometry is very complex. CFD provides an alternative method, which is reliable and less expensive to study the flow behaviour inside the ESP. An accurate CFD model plays an important role in predicting the flow field characteristics inside the ESP and optimizing flow distributions within the ESP by simulating proposed modifications. This ensures that the desired flow profiles are achieved, thus substantially reducing the outage time. However, only a limited number of research could be found in the literature for the prediction of turbulent flow behavior inside the ESP. Dumont and Mudry [4] made a comparative study on flow simulation results obtained from different precipitator CFD models. Other researchers are focused on 2D ESP models based on simplified geometrical arrangements and ignored the effect of sudden expansion in geometrical configuration of an ESP. Zhao et al. [5] developed a simple 2D model which consists of a single discharge wire and two parallel plates. The 2D model developed by Skodras et al. [6] consists of three wires and two parallel plates arrangements. Nikas *et al.* [7] simulated a 3D flow inside a laboratory scale precipitator of three-wire and two-plate arrangements. Varonos et al. [8] developed a 3D model and introduced smoothing grids to improve the flow characteristic of an ESP. But they simplified their model by introducing a porous region instead of creating any physical collecting plates in their model. The numerical flow model of an ESP developed by Schwab and Johnson [9] replaced all the collection plates inside the ESP with equivalent resistance. Gallimberti [10] also used local loss coefficients in the governing equations to model the different wall profiles and other structures inside the ESP.

The above studies were found to simulate fluid flow inside the ESP with either simplified models or simplified geometries. The accurate aerodynamic characteristics of the flow inside an ESP in an operation may not be obtained without considering all of its major physical details. The novelty of this study is to develop a new 3D fluid flow model

Manuscript submitted October 29, 2006; Revised version submitted March 29, 2007.

Shah M. E. Haque is with the Process Engineering & Light Metals (PELM) Centre, Faculty of Sciences, Engineering and Health, Central Queensland University, Gladstone, Queensland 4680, AUSTRALIA (corresponding author to provide phone: +61-413792234; fax: +61-7-49309382; e-mail: s.haque@cqu.edu.au).

M. G. Rasul is a Senior Lecturer in Mechanical Engineering, College of Engineering and Built Environment, Faculty of Sciences, Engineering and Health, Central Queensland University, Rockhampton, Queensland 4702, AUSTRALIA (e-mail: m.rasul@cqu.edu.au).

M. M. K. Khan is an Associate Professor and Head of Department of Infrastructures in the Faculty of Sciences, Engineering and Health, Central Queensland University, Rockhampton, Queensland 4702, AUSTRALIA (e-mail: m.khan@cqu.edu.au).

A. V. Deev is with the Process Engineering & Light Metals (PELM) Centre, Faculty of Sciences, Engineering and Health, Central Queensland University, Gladstone, Queensland 4680, AUSTRALIA (e-mail: a.deev@cqu.edu.au).

N. Subaschandar was with the Process Engineering & Light Metals (PELM) Centre, Faculty of Sciences, Engineering and Health, Central Queensland University, Gladstone, Queensland 4680, AUSTRALIA (e-mail: s.rao@cqu.edu.au).

using CFD code FLUENT of a lab scale ESP which considers all of its major physical features. It is to be noted that all the collecting electrodes (CE), baffles, gas deflectors etc. are taken into account in this CFD model and have not been replaced by any equivalent porous region as other researchers have done in their studies. A detailed numerical approach and simulation procedure is presented for the prediction and optimization of the flow distribution inside the ESP. The predicted results are compared with the laboratory measured data. The model developed for the ESP has the potential to better predict the effect of possible modifications on flow optimization.

## II. EXPERIMENTAL SET UP AND PROCEDURES

### A. ESP configuration

The lab-scale ESP was geometrically similar to the ESP used at a local power station. The detail geometry of the power station's ESP was presented elsewhere [11], [12]. The dimension of the lab scale model was reduced by 20 times from the original dimension of the full scale ESP. The geometrical details of the lab-scale ESP are presented in Fig. 1. The model consisted of a rectangular collection chamber, an inlet evase and an outlet evase. The effective length, width and height of the collection chamber are 1.518 m, 0.655 m and 0.55 m respectively. The inlet evase is a pyramidal diffuser with large divergence angle (more than  $50^\circ$ ) which is located in front of the collection chamber. The outlet evase, which is a convergent duct, is located after the collection chamber. One perforated plate with 62% opening and two perforated plates with 69% openings were placed inside the inlet evase. Another perforated plate with 62% opening was placed inside the outlet evase. Four sets of collection plates were placed inside the collection chamber. The plates were placed 2 cm apart. Acrylic material was chosen because of its better optical clarity to enable precise visual observation. The total test rig was placed in a wind tunnel with appropriate duct arrangements (Fig. 2). Due to the symmetry in geometry only one-half of the physical model was considered for the simulation purpose.

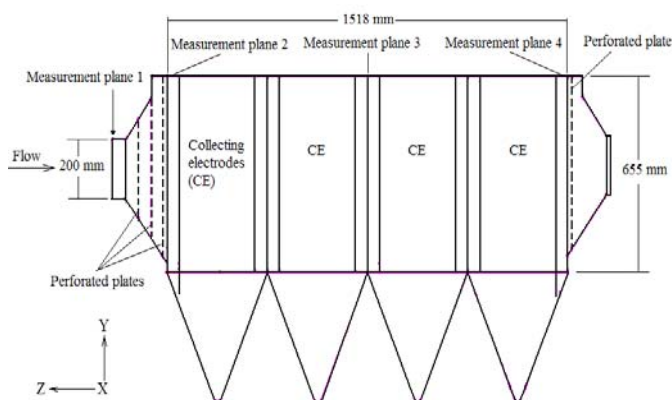


Fig. 1 Schematic diagram of the lab-scale ESP

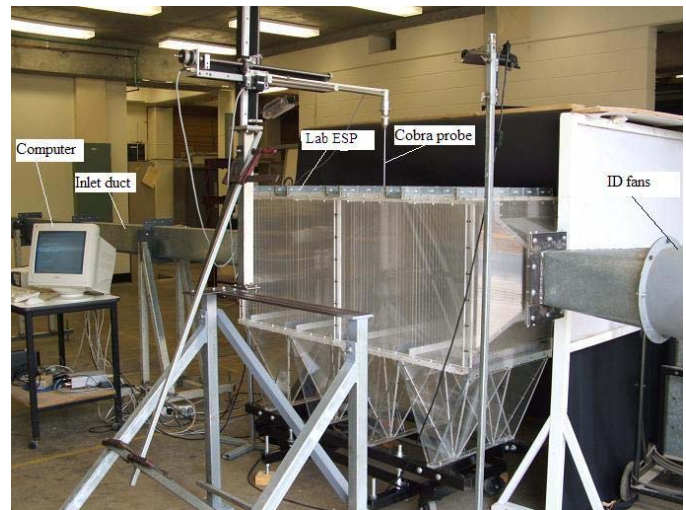


Fig. 2 Experimental set up

### B. Experimental procedures

The measurement of velocity was done inside the duct at plane 1 and inside the ESP at plane 2, 3 and 4 (Fig. 1) with the induced-draft fans operating at 3000 rpm motor speed. The mean speed of the air flow was approximately 30.6 m/s, measured at plane 1 which corresponds to a Reynolds number of  $Re = 3 \times 10^5$  based on the hydraulic diameter of the inlet duct. The tests were performed at atmospheric pressure (764 mm Hg) and room temperature ( $26^\circ\text{C}$ ) condition. A cobra probe made by Turbulent Flow Instrumentation [13], an Australian company was used to measure the flow inside ESP.

The Cobra Probe, as shown in Fig. 3 is a 4-hole pressure probe that provides dynamic, 3-component velocity and local pressure measurements in real-time. The Cobra Probe incorporates four 0.5 mm pressure taps in a multi-faceted head, with the pressure taps connected via tubing to pressure transducers in the body of the Probe. The Cobra Probe was supplied fully calibrated and ready to use. TFI's Windows-based 'Device control' software provided a powerful, easy-to-use interface for controlling and operating the cobra probe.



Fig. 3 Four-hole Cobra probe

Flow visualization was done to check the direction of flow inside the physical model. A digital camera and a video camera were used for this purpose. Smoke was used as tracer medium.

### III. NUMERICAL APPROACH AND SIMULATION PROCEDURE

Numerical computation of fluid transport includes conservation of mass, momentum and turbulence model equations. The Fluent Inc. geometry and mesh generation software “Gambit” was used as a preprocessor to create the geometry, discretize the fluid domain into small cells to form a volume mesh or grid and set up the appropriate boundary conditions. The flow properties were then specified, the equations were solved and the results were analyzed by “Fluent” solver.

#### A. Governing equations

The basis of modeling of an incompressible Newtonian fluid flow module is the use of the conservation of mass equation [14] given by,

$$\frac{\partial \rho}{\partial t} + \bar{\nabla} \cdot (\rho \bar{U}) = 0 \tag{1}$$

and the momentum equation [14] given by,

$$\frac{\partial \bar{U}}{\partial t} + \bar{U} \cdot \bar{\nabla} \bar{U} = -\frac{\bar{\nabla} p}{\rho} + \nu \bar{\nabla}^2 \bar{U} + \bar{g} \tag{2}$$

For the turbulent flow inside the ESP, the key to the success of CFD lies with the accurate description of the turbulent behavior of the flow. To model the turbulent flow in an ESP, there are a number of turbulence models available in Fluent. The realizable  $k-\varepsilon$  model is a relatively recent development and contains a new formulation for the turbulent viscosity and a new transport equation for the dissipation rate,  $\varepsilon$  which can be written as follows [15],

$$\frac{\partial}{\partial t}(\rho k) + \frac{\partial}{\partial x_j}(\rho k u_j) = \tag{3}$$

$$\frac{\partial}{\partial x_j}[(\mu + \frac{\mu_t}{\sigma_k}) \frac{\partial k}{\partial x_j}] + G_k + G_b - \rho \varepsilon - Y_M + S_k$$

$$\frac{\partial}{\partial t}(\rho \varepsilon) + \frac{\partial}{\partial x_j}(\rho \varepsilon u_j) = \tag{4}$$

$$\frac{\partial}{\partial x_j}[(\mu + \frac{\mu_t}{\sigma_\varepsilon}) \frac{\partial \varepsilon}{\partial x_j}] + \rho C_1 S \varepsilon - \rho C_0 \frac{\varepsilon^2}{k + \sqrt{\nu \varepsilon}} +$$

$$C_{1\varepsilon} \frac{\varepsilon}{k} C_{3\varepsilon} G_b + S_\varepsilon$$

Where,

$$C_1 = \max[0.43, \frac{\eta}{\eta + 5}], \quad \eta = S \frac{k}{\varepsilon}, \quad S = \sqrt{2 S_{ij} S_{ij}}$$

The turbulence intensity, which is defined as the ratio of the root-mean-square of the velocity fluctuations, to the mean

flow velocity can be estimated from the following formula derived from an empirical correlation for pipe flows [15],

$$I = \frac{u'}{u_{avg}} = 0.16 (Re_{Dh})^{-1/8} \tag{5}$$

A source term was added to the  $k-\varepsilon$  turbulence model equations to estimate the pressure drop across the perforated plates. In the CFD simulation, the perforated plates are modeled as thin porous media of finite thickness with directional permeability over which the pressure change is defined as a combination of viscous loss term and an inertial loss term and is given by [15],

$$\Delta p = -(\frac{\mu}{\alpha} U + C_2 \frac{1}{2} \rho U^2) \Delta m \tag{6}$$

Haque et al. [16] found from their study that the pressure drop across the perforated plate is mainly due to the inertial loss at turbulent flow condition. The viscous loss term was eliminated from (6) due to this reason. Appropriate values for  $C_2$  were then calculated from the literature [17].

#### B. Boundary conditions

The finite volume method was used to discretize the partial differential equations of the model using the SIMPLEC method for pressure-velocity coupling and the second order upwind scheme to interpolate the variables on the surface of the control volume. The segregated solution algorithm was selected to solve the governing equations sequentially (i.e., segregated from one another). Standard wall functions, which are a collection of semi-empirical formulas and functions, were applied to bridge the viscosity-affected region between the wall and the fully-turbulent region. The wall function approach is a popular and practical option for the near-wall treatments for industrial flow simulations. The inlet boundary condition of the model was set as an inlet velocity profile by using a set of velocity measured at 27 point inside the duct at plane 1 (Fig. 1) of ESP. The direction of the velocity was normal to the inlet boundary. The turbulent intensity at the inlet boundary was set as 3%, based on the Reynolds number of the flow ( $Re = 3.1 \times 10^5$ ) and calculated using (5). An atmospheric pressure boundary located downstream of the outlet duct was specified as pressure-outlet. The pressure-outlet boundary was placed far away from the outlet evase so as not to affect the flow inside the ESP. The no-slip boundary condition was used in all the walls. Porous jump boundary condition was used for the perforated plates.

### IV. RESULTS AND DISCUSSIONS

The CFD model of the ESP (Fig. 4) consists of about 1.2 million computational nodes. The grid independency was checked and the simulation was performed with a Pentium IV 3.2 GHz 32bit CPU workstation with 2GB RAM-memory and 80 GB hard disc memory. A converged solution was obtained after approximately 1500 iterations.

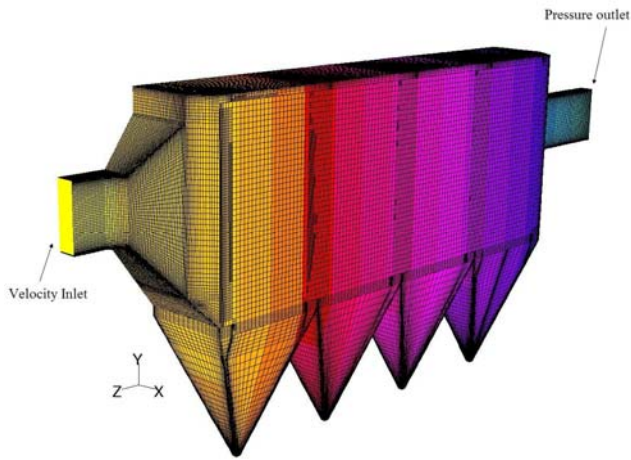


Fig. 4 Computational grid of ESP model

The predicted velocities at height  $y = 0.36$  m of plane 2, 3 and 4 as shown in Fig. 1 are compared with the measured velocity. Flow visualization was done before commencing the measurement. Flow visualization revealed vortices and flow separation in some areas particularly near the wall at plane 3 and 4 of the ESP as is shown in Fig.5. No measurements were carried out near the wall at those planes, since correct measurements can not be achieved by using cobra probe in the presence of vortices. The simulation also revealed the existence of vortices near the wall regions.

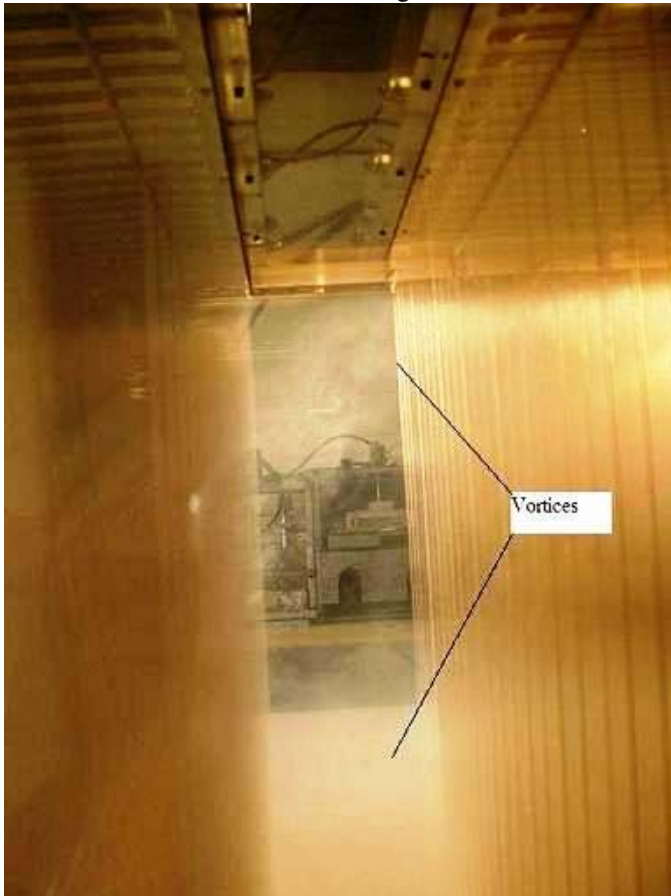


Fig.5 Flow visualization picture showing vortices inside the ESP

Figs. 6, 7 and 8 present the velocity comparison at the three measurement planes, which give a reasonably good prediction with a maximum deviation of about 10% on the measured values.

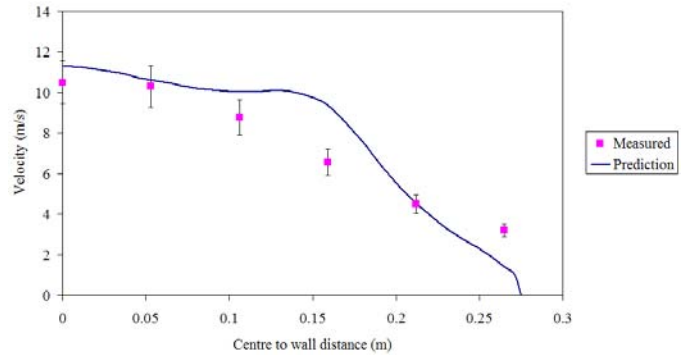


Fig. 6 Velocity distribution from centre to wall at  $y = 0.36$  m (plane 2) – Comparison between the measured data and CFD prediction

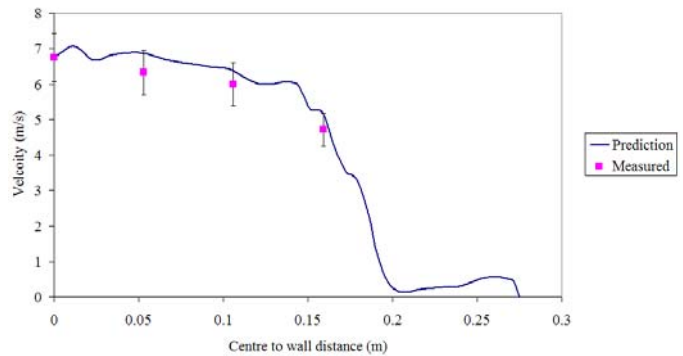


Fig. 7 Velocity distribution from centre to wall at  $y = 0.36$  m (plane 3) – Comparison between the measured data and CFD prediction

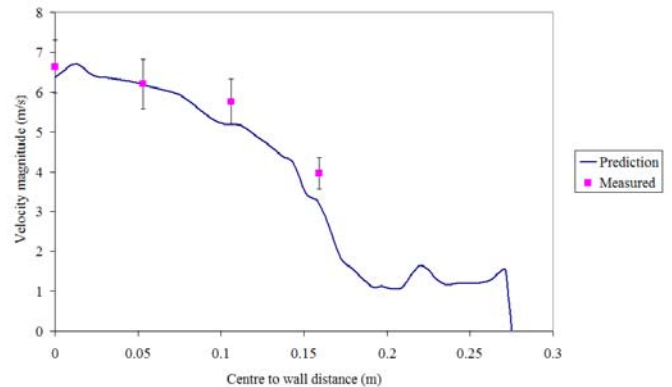


Fig. 8 Velocity distribution from centre to wall at  $y = 0.36$  m (plane 4) – Comparison between the measured data and CFD prediction

It is seen that the prediction lines are not as smooth as they usually appear in flows through ducts or pipes. This is due to the influence of the plates and other geometries which are fitted in the ESP. The velocity distribution is found affected by the swirling flow phenomena near the wall region arising as a result of flow separation. Concave velocity distributions are noticed near the wall region (Fig. 7 and 8). Kito and Kato

[18] found a similar type of concave flow pattern in the swirling flow region in a pipe.

This 3D fluid flow model which is validated by the measured data should give a good prediction of the effects of geometrical modification on optimizing flow distribution inside the ESP. The velocity contour at  $y = 0.36$  m of the developed CFD model is presented in Fig. 9 which shows a low velocity region near the wall. The velocity vectors presented in Fig. 10 showed that the velocity distributions were not uniform inside the ESP at the current setup.

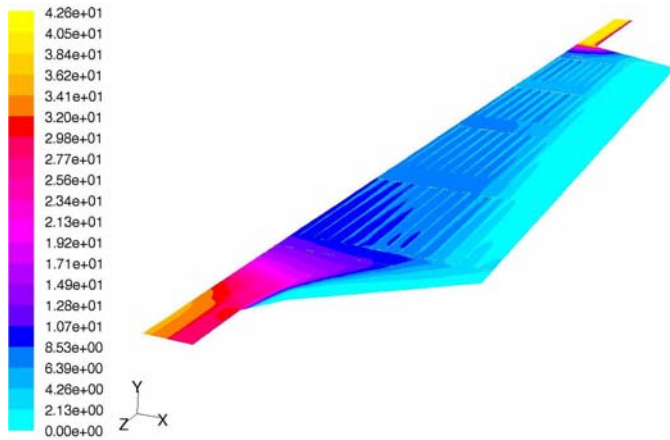


Fig. 9 Velocity contours at  $y = 0.36$  m – plan view section (before modification)

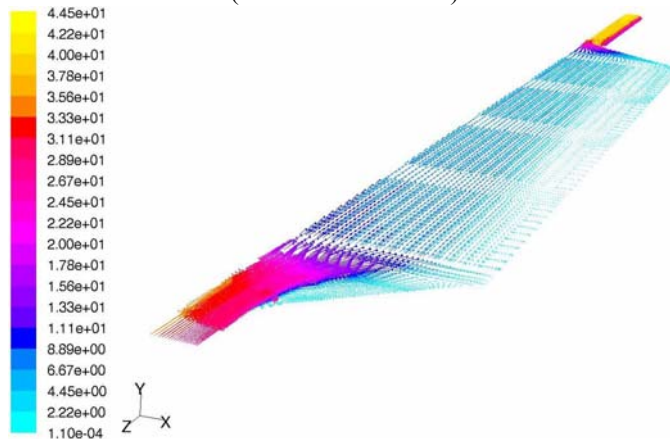


Fig. 10 Velocity vectors at  $y = 0.36$  m – plan view section (before modification)

The model was modified to remove the non uniformity by changing the value of  $C_2$  of the porous-jump boundary condition. The modified boundary conditions were found to create desired resistance over the cross section and regulate the flow in both the diffuser and the channel following it. Fig. 11 and 12 present the velocity contours and the velocity vectors of the modified model respectively where the results show that the flow is more uniformly distributed now.

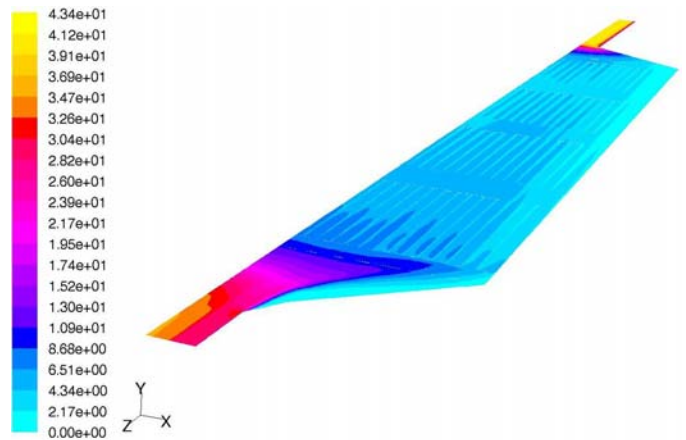


Fig. 11 Velocity contours at  $y = 0.36$  m – plan view section (after modification)

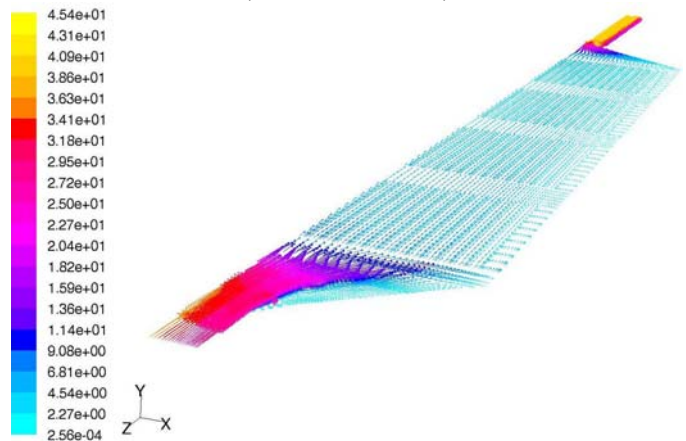


Fig. 12 Velocity vectors at  $y = 0.36$  m – plan view section (after modification)

The procedure and technique adopted here to optimize the flow distribution inside the lab-scale ESP was applied successfully to develop a flow model of an ESP of a power plant. The modeling details and results were illustrated elsewhere (Haque et al. 2007).

### V. CONCLUDING REMARKS

A fluid flow model of a laboratory scale ESP, including its major physical features, is developed using CFD code FLUENT. Realizable  $k-\epsilon$  turbulence model was used for computing turbulence parameters inside the ESP. Numerically predicted velocity profiles inside the ESP are compared with the measured data. These predictions are found to be in reasonable agreement with the measured data. The model developed is found useful to predict an improved flow pattern inside the ESP by introducing modifications in the ESP designs. This modeling procedure can be applied to model any full scale ESP.

### NOMENCLATURE

$C_0, C_{1\epsilon}, C_{3\epsilon}$	Constants
$C_2$	Pressure jump coefficient = Pressure loss coefficient per unit thickness ( $m^{-1}$ )

$g$	Gravity ( $\text{m/s}^2$ )
$G_k$	Generation of turbulence kinetic energy due to the mean velocity gradients ( $\text{m}^2/\text{s}^2$ )
$G_b$	Generation of turbulence kinetic energy due to buoyancy ( $\text{m}^2/\text{s}^2$ )
$I$	Intensity
$k$	Turbulent kinetic energy ( $\text{m}^2/\text{s}^2$ )
$\Delta m$	Thickness of the perforated plate (m)
$p$	Pressure (Pa)
Re	Reynolds number
$U$	Velocity (m/s)
$S_k, S_\varepsilon$	User-defined source terms
$S$	Modulus of the mean rate of strain tensor
$u'$	Fluctuating velocity (m/s)
$u_{avg}$	Average velocity (m/s)
$Y_M$	Contribution of the fluctuating dilatation in compressible turbulence to the overall dissipation rate

*Greek symbols*

$\alpha$	Permeability of the perforated plate ( $\text{m}^2$ )
$\Delta$	Differential
$\varepsilon$	Turbulent dissipation rate ( $\text{m}^2/\text{s}^3$ )
$\eta$	Strain
$\mu$	Dynamic viscosity ( $\text{N.s/m}^2$ )
$\nu$	Kinematic viscosity ( $\text{m}^2/\text{s}$ )
$\rho$	Density ( $\text{kg/m}^3$ )
$\sigma_k$	Turbulent Prandtl numbers for $k$
$\sigma_\varepsilon$	Turbulent Prandtl numbers for $\varepsilon$

*Subscripts*

Dh	Hydraulic diameter
----	--------------------

## REFERENCES

- [1] M. G. Rasul, W. Widiyanto and B. Mohanty, "Assessment of the thermal performance and energy conservation opportunities in cement industry in Indonesia", *Applied Thermal Engineering*, vol. 25, pp. 2950 – 2965, 2005.
- [2] M. G. Rasul, B. S. Tanty and B. Mohanty, "Modeling and analysis of blast furnace performance for efficient utilization of energy", *Applied Thermal Engineering*, vol. 27, pp. 78 – 88, 2007.
- [3] Anatol Jaworek, Andrzej Krupa and Tadeusz Czech, "Modern electrostatic devices and methods for exhaust gas cleaning: A brief review", *Journal of Electrostatics*, vol. 65, pp. 133 – 155, 2007.
- [4] B. J. Dumont and R. G. Mudry, "Computational fluid dynamic modeling of electrostatic precipitators", *Proceedings of electric power conference*, 2003.
- [5] L. Zhao, E. Dela Cruz, K. Adamiak, A. A. Berezin and J. S. Chang, "A numerical model of a wire-plate electrostatic precipitator under electrohydrodynamic flow conditions", *CD – ROM proceedings of the international conference on air pollution abatement technologies-Future challenges*, Cairns, Australia, 2006.
- [6] G. Skodras, S. P. Kalidas, D. Sofialidis, O. Faltsi, P. Grammelis and G. P. Sakellariopoulos, "Particulate removal via electrostatic precipitators – CFD simulation", *Fuel Processing Technology*, vol. 87, pp. 623 – 631, 2006.
- [7] K. S. P. Nikas, A. A. Varnos and G. C. Bergeles "Numerical simulation of the flow and the collection mechanisms inside a laboratory scale electrostatic precipitator", *Journal of Electrostatics*, vol. 63, pp. 423-443, 2005.

- [8] A. A. Varnos, J. S. Anagnostopoulos and G. C. Bergeles, "Prediction of the cleaning efficiency of an electrostatic precipitator", *Journal of Electrostatics*, vol. 55, pp. 111 – 133, 2002.
- [9] M. J. Schwab and R. W. Johnson, "Numerical design method for improving gas distribution within electrostatic precipitators", *Proceedings of the american power conference*, vol. 56(1), pp. 882-888, 1994.
- [10] I. Gallimberti, "Recent advancements in the physical modeling of electrostatic precipitators", *Journal of Electrostatics*, vol. 43, pp. 219-247, 1998.
- [11] S. M. E. Haque, M. G. Rasul, A. Deev, M. M. K. Khan and J. Zhou, "Numerical simulation of turbulent flow inside the electrostatic precipitator of a power plant", *WSEAS Transactions on Fluid Mechanics*, vol. 1(1), pp. 96 – 101, 2006.
- [12] S. M. E. Haque, M. G. Rasul, A. Deev, M. M. K. Khan and J. Zhou, "The influence of flow distribution on the performance improvement of electrostatic precipitator", *CD – ROM proceedings of the international conference on air pollution abatement technologies-Future challenges*, Cairns, Australia, 2006.
- [13] Turbulent Flow Instrumentation (TFI) Pty Ltd. (2005) <http://www.turbulentflow.com.au>
- [14] B. R. Munson, D. F. Young and T. H. Okiishi, *Fundamentals of fluid mechanics*, 4<sup>th</sup> ed, John Wiley & Sons Inc., NewYork, 2002.
- [15] *Fluent 6.2 User's Guide*, Fluent Inc., 2005.
- [16] S. M. E. Haque, M. G. Rasul, M. M. K. Khan, A. V. Deev and N. Subaschandar, "Flow distribution inside an electrostatic precipitator: effects of uniform and variable porosity of perforated plate", *Proceedings of the 5<sup>th</sup> WSEAS/IASME international conference on heat transfer, thermal engineering and environment*, Athens, 2007, pp. 61 – 66.
- [17] I. E. Idelchik, *Handbook of hydraulic resistance*, 3<sup>rd</sup> ed, CRC Press Inc., 1994.
- [18] O. Kito and T. Kato, "Near wall velocity distribution of turbulent swirling flow in circular pipe", *Bulletin of JSME*, vol. 27(230), pp. 1659 – 1666, 1984.

**Shah M. E. Haque** received his Bachelor of Science in Mechanical Engineering from Bangladesh University of Engineering and Technology (BUET), Dhaka, Bangladesh in 1998.

Currently he is doing his PhD on Process and Resource Engineering at the Process Engineering and Light Metals (PELM) Centre, Faculty of Sciences, Engineering and Health, Central Queensland University, Gladstone, Queensland 4680, Australia.

His research activities are in the area of fluid mechanics, computational fluid dynamics (CFD), process engineering and environmental pollution control. He is one of the reviewers of World scientific and engineering academy and society (WSEAS).

**Mohammad G. Rasul** graduated in Mechanical Engineering from Bangladesh University of Engineering and Technology (BUET), Dhaka, Bangladesh in 1987. He completed his Master of Engineering in Energy Technology from Asian Institute of Technology (AIT), Bangkok, Thailand, in 1990. He obtained PhD on Energy and Thermodynamics from The University of Queensland, Australia, in 1996.

Currently, he is working as a Senior Lecturer in Mechanical Engineering at College of Engineering and the Built Environment, Faculty of Sciences, Engineering and Health, Central Queensland University, Rockhampton, Queensland 4702, Australia. He is specialised and experienced, and interested in research, teaching and consultancy in the area of thermodynamics and energy, fluid mechanics, process industry's energy and environmental pollution analysis and building energy analysis.

Dr Rasul is an author of more than 80 refereed journal and conference papers including few chapters in books. He is an active member of the Engineers Australia and the Australasian Association for Engineering Education

**M. Masud K. Khan** is an Associate Professor and Head of Department of Infrastructures in the Faculty of Sciences, Engineering and Health, Central Queensland University, Rockhampton, Queensland 4702, Australia. He received his MS (Mech) with 1st class Honours from Moscow Institute of Petrochemical and Gas Industry in 1982. Subsequently he worked with the oil industry for 2 years. He obtained his PhD in engineering from the University of Sydney in 1990.

His teaching, research and consulting activities are in the area of non-Newtonian fluid mechanics, thermofluid engineering and rheology of industrial fluids and polymeric materials.

He has authored more than 95 refereed journal, conference and technical papers. He is a member of American Society of Rheology, Australian Society of Rheology, Engineers Australia and the Australasian Association for Engineering Education (AAEE).